Towards a periodic deterministic source of arbitrary single-photon states

To cite this article: Evan Jeffrey et al 2004 New J. Phys. **6** 100

View the article online for updates and enhancements.

New Journal of Physics

Towards a periodic deterministic source of arbitrary single-photon states

Evan Jeffrey, Nicholas A Peters and Paul G Kwiat

Department of Physics, University of Illinois at Urbana-Champaign, Urbana, IL 61801, USA

E-mail: ejeffrey@uiuc.edu, npeters@uiuc.edu and kwiat@uiuc.edu

Abstract. We present an experimentally feasible scheme to create single photons *deterministically* out of a non-deterministic spontaneous parametric downconversion source. We give an efficiency analysis of obtaining exactly one photon in the output. Furthermore, we experimentally demonstrate a way to control the purity of an output photon using a partial measurement of a polarization-entangled photon pair, a partial implementation of remote state preparation. When combined, these two techniques could allow on-demand preparation of single photons in arbitrary states.

Contents

1. Introduction

Quantum information processing is now known to enable a variety of remarkable feats which are impossible with systems limited to the laws of classical physics. These feats include provably secure encryption of information [1], teleportation [2] and exponential speed-up in the implementation of certain computational algorithms [3]. Some of the greatest progress so far in the field has taken place in the area of quantum communications, where quantum bits—qubits—are encoded, e.g. in the polarization states of single photons. Nevertheless, there remains a great deal of work to be done in the development of quantum photonic technologies to enable practical implementation of these ideas. One such requirement is that of a light source which produces single photons on demand, i.e. producing a close approximation of the Fock state $|1\rangle$. Such a source would be extremely useful for quantum cryptography, which implicitly assumes that bits of a key are transmitted using true single-photon states, as multiple photons can leak information to a potential eavesdropper. Single-photon sources are also a key resource to enable scalable quantum computing with linear optics [4]. In addition, there are a number of other applications which would benefit from such sources, including detector calibration for low-light level radiometry, and even studies of the optical response of biological systems to single photons.

A variety of experimental approaches are being pursued to realize single-photon sources. Many of them involve the excitation of a single quantum emitter, which by definition can then release at most one photon. These systems include quantum dots [5], nitrogen vacancies in a diamond lattice [6] and single atoms or ions coupled with a high-finesse cavity [7, 8]. One challenging aspect of all these approaches is that it is nontrivial to constrain the photon to be emitted into a desirable spatial mode, as is most useful for many applications. For this reason, the maximum out-coupling efficiency has still been rather low (less than 40%) with these sources [9]. In this paper, we described a rather different approach to realizing single-photon sources via the process of spontaneous parametric downconversion (SPDC) [10]–[13].

2. 'Heralded' photons from downconversion

The SPDC process is essentially the inverse of second-harmonic generation: a nonlinear crystal, such as BBO, is pumped by a laser to produce pairs of correlated lower-energy photons, historically called the 'signal' and the 'idler'. Contingent on detecting a photon in the idler mode, the quantum state of the signal mode closely approximates an exact single-photon state [11], i.e. detection of the idler photon 'heralds' the presence of a single photon in the signal mode. This approximation is valid as long as the probability of detecting at least one photon (within the time resolution of the detector) is much less than one, which has usually been the case in previous experiments.

The SPDC-based photon source has a number of useful characteristics. The created pair of photons must conserve the energy and momentum of the parent pump photon (the 'phase-matching' conditions), allowing useful control of the spatial mode and bandwidth of the generated photons. In fact, the signal and idler photons are always entangled in these degrees of freedom. The energy entanglement constrains the wavelength of the signal photon once the wavelength of the idler is determined (usually by passing through a narrow bandpass filter); in addition, the relative emission times are tightly constrained by sub-picosecond time correlations. Similarly,

the momentum entanglement implies that detection of the idler photon can be used to prepare the signal in a well-defined spatial mode.

The main drawback of the SPDC-based single-photon source is low efficiency [13]. In a synchronous system (i.e. using a pulsed pump laser) most input pulses will generate no downconversion pairs at all. The idler detector will not fire, and the cycle will be wasted. This may be acceptable for applications only requiring heralded sources, but others, such as scalable linear optics quantum computation [4], require on-demand or at least predictable generation of single photons. Increasing the crystal length or pump power will increase the efficiency, but it must be kept low enough that the probability of two downconversion events (essentially following the Poisson statistics) is very small. Otherwise, detection of an idler photon may herald the arrival of two signal photons in a single pulse. Such multi-photon states are undesirable for many quantum information processing tasks. For example, in quantum cryptography, an eavesdropper can use the extra photon to gain information about the key being generated without alerting the sender and receiver to her presence.

3. Deterministic source

Pittman *et al* [12] implemented the idea of using the trigger detection to switch the signal photon into a storage cavity, to be released at some later time. Our scheme extends and improves on this approach. Specifically, as shown in figure 1, instead of sending a single pump pulse for every output cycle, we will use a burst of pulses to pump the downconversion crystal. Employing multiple pump pulses in this way can greatly reduce the multi-photon probability. If sufficiently many pulses are used, the probability that at least one will generate a downconversion pair can be made high while keeping the probability of double pairs in a *single* pulse small. This is the crucial difference that should allow this source to work better than the simple heralded source—a single photon in any one pulse within a burst is sufficient to generate an output signal photon, but multiple photon pairs are only problematic if they spawn from the same input pulse.[1] In this case, if only one of the trigger photons is detected, it is possible to output more than one photon in a single pulse. We can reduce this possibility somewhat by using multiple detectors in a tree configuration (as indicated in figure 1). By increasing the number of detectors in the array, it is probable that two photons from a multi-photon pulse will go to different detectors and both be detected. In this case the signal photon is discarded.

Once the candidate signal photon is identified by the detection of its idler 'partner' photon, it is directed into a switchable delay line that can be opened and closed to hold the photon until it is released at the end of the cycle. Thus, we can convert an intrinsically nondeterministic process into one that is periodic at the cost of a reduced output rate, e.g. 1 photon per 20 input pulses. Neglecting losses, the success probability of generating exactly one photon will improve as the number of input pulses per cycle is increased, nearing 100% with only a small probability of generating more than one photon. In practice, losses reduce the final single-photon probability, so that, for a given loss, there is an optimal number of cycles.

---

[1] Migdall *et al* [13] propose to achieve the same advantage in a conceptually similar system using *space* multiplexing instead of time: the pump is split between several branches, each of which contains a downconversion crystal and a trigger detector. The signal mode of these branches are recombined using an electro-optic switchyard, conditional on which trigger detectors fired. Although, in principle, this achieves the same effect as our scheme, it requires substantially more hardware, i.e. nonlinear crystals and detectors, in addition to the fast low-loss switchyard.
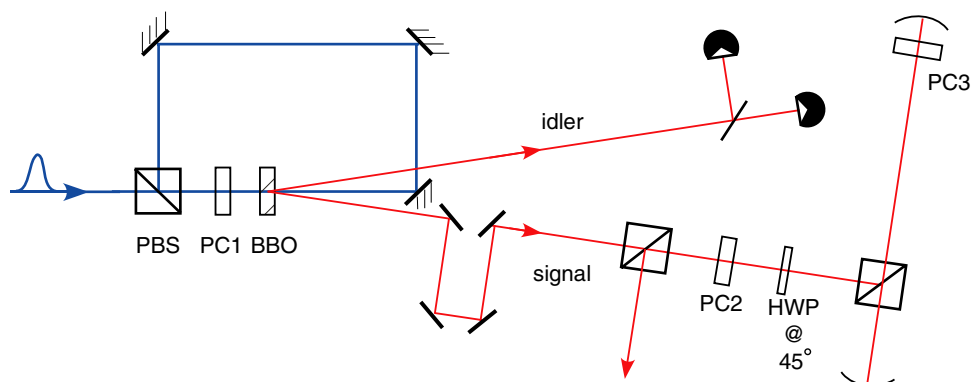
Figure 1. Set-up to generate single photons on demand. A single incident pump pulse of horizontal polarization is converted to vertical polarization by Pockels cell PC1. It then has some probability to produce 1 (or more) photon pairs via the process of spontaneous parametric downconversion each time it passes through the nonlinear crystal (shown here as BBO). Detection of the idler photon allows the signal photon to be switched into the storage loop. Multiple detectors in the idler branch allow some rejection of multiple-pair events, reducing the likelihood of generating two output photons instead of one. The signal photon is initially horizontally polarized, then rotated to vertical by the HWP before the storage loop. The loop is switched by rotating the signal photon's polarization with a Pockels cell (PC3) to horizontal polarization, so it stays within the cavity. At the end of the cycle, the polarization is rotated back to vertical and the polarizing beam splitter (PBS) reflects the signal photon back into free space. PC2 is another Pockels cell used to undo the effect of the HWP, and thus switch the photon out of the path of the initial downconversion. This prevents other downconversion events from being seen at the output, and prevents the output from returning through the nonlinear crystal. An animated version of this figure showing its operation is available online.

4. Efficiency

There are at least four relevant numbers that quantify how effective a single-photon source is. The first is the probability of success—the probability of producing exactly one photon in a given output pulse. The other three are the probabilities of the various failure modes which are: no trigger photon is detected, a trigger photon is detected but the output is still empty, and two or more photons are present in one output pulse. The experimental parameters that govern these probabilities are downconversion efficiency (a combination of pump power and crystal thickness that controls the average rate of downconversion), the number of detectors in the trigger photon arm (which affects how well multi-photon pulses can be discriminated), the detector efficiency, the length of the pump pulse train (i.e. the number of pulses per attempt) and the storage loop efficiency (in turn dependent on the losses in the mirrors and switch-out elements).

To analyse the system we represent the array of inefficient detectors by a single loss element followed by an array of perfect detectors. This is trivial in the case of perfectly matched detectors with efficiency q—we simply model the idler arm as a neutral density filter with transmission q

followed by the same tree of perfectly efficient detectors. If the detectors are of unequal efficiency, this can still be done [14], but will not be considered here.

The total probability of emitting x photons from the system in a given cycle is given by the general equation

$$p(x) = \sum_{i=1}^{n} \left(1 - \sum_{k=1}^{n} create(k) \cdot detect(1|k) \right)^{i-1} \sum_{k=1}^{\infty} create(k) \cdot detect(1|k) \cdot emit(x|k). \tag{1}$$

The term $create(k)$ is the probability a single pulse gives k output pairs; $detect(m|k)$ is the probability of detecting m idler photons from a single pulse, conditional on k created pairs; and $emit(x|k)$ is the probability of emitting x signal photons, conditional on k created pairs. Thus, the first part of equation (1) is the probability that the first $i-1$ pump pulses did *not* result in a single idler photon detection and, therefore, the storage apparatus was never triggered. That factor is multiplied by the probability of detecting one photon and emitting x photons on pump pulse i, and the entire quantity summed over each pump pulse to give the total probability of emitting x signal photons. If this equation is also summed over all values of x, we find the value is less than unity. The remaining probability is the chance that the idler detectors are never triggered, and there is neither a trigger nor an output pulse. The value of $p(0)$ from the above equation denotes the probability that a pair is created, but the signal photon is lost before reaching the output.

The form of the generic terms in equation (1) is relatively easy to derive. $create(k)$ is a Poissonian distribution:

$$create(k) = P_\lambda(k) = \frac{e^{-\lambda} \lambda^k}{k!}, \tag{2}$$

where λ is the mean number of pairs per pump pulse, governed by the pump power and crystal length,

$$emit(x|k) = (\eta^{n-i})^x (1 - \eta^{n-i})^{(k-x)} \binom{k}{x}, \tag{3}$$

where η^{n-i} is the efficiency of the storage loop when it must hold the signal for the remaining $n-i$ pump pulses, and

$$detect(1|k) = \sum_{l=1}^{k} q^l (1-q)^{(k-l)} \binom{k}{l} \left(\frac{1}{D} \right)^{l-1}. \tag{4}$$

Here, q is the detector efficiency and D is the number of detectors. Thus, the probability of detecting exactly one idler photon is the sum over l, the number of photons that would be detected with ideal number-counting detectors, multiplied by the probability $(1/D)^{l-1}$ that all l idlers go to the same detector, thereby only being counted once.

Finally, we must take into account the mode collection efficiency. Since the downconverted photons must conserve momentum inside the crystal, they are tightly constrained in direction—in principle, detecting the location of the idler projects the signal into a well-defined spatial mode. The accuracy of the spatial correlations depends intrinsically on the geometry of the crystal and the spatial mode of the pump. The conditional detection probability of the signal photon also depends on the measurement conditions for the trigger photon, i.e. the collection optics and any spectral filtering [13], [15]–[17]. In practice, the collection modes for the two branches will not

be perfectly aligned. In this case, there is a possibility that we will detect an idler photon, but the signal photon will not be in the collection mode of the storage loop. These 'false positives' are equivalent to a fixed attenuation of the output beam. Similarly, it is possible for signal photons to be generated in the correct collection mode but for the idler trigger to miss the collection aperture of the detector. This effect is roughly equivalent to lowering the detector efficiency q. Obviously, it is important to maximize the mode overlap between the signal and the idler to achieve the best system performance.

5. Implementation

There are three key areas of the implementation: the downconversion source itself, the detector array and the switchable storage loop. The downconversion source is similar to that of the heralded source. The pump laser is chosen to allow the trigger photon wavelength to be near the peak detection efficiency of Si avalanche photodiodes (APD), ~700 nm. The nonlinear crystal is chosen for the pump wavelength and phase-matching conditions desired, with BBO a common choice for UV pumps. In our system, the pump is a frequency-tripled Nd:YAG laser which produces sub-nanosecond pulses at 355 nm with peak intensities above 10 kW; the crystal is cut to generate 702 nm (signal) and 718 nm (idler) photon pairs in a noncollinear arrangement.[2] We recycle a single large pump pulse to generate the required burst of pulses as shown in figure 1. If we do not recycle the pump, we must either be able to store the signal photons for a longer time (e.g. a 10 kHz repetition rate Q-switched pump laser would require a 100 μs storage), or we must have an extremely high-average pump power. The length of the recycling loop dictates the time between attempts, which must be at least long enough to allow the Pockels cell (PC3 from figure 1) to cleanly select a single pulse, while excluding downconversion generated by adjacent pulses. The minimum on-time for a bulk Pockels cell is typically 10 ns, requiring the base length of the storage loop to be about 2 m.

Detection of the idler photon as a trigger is done by one or more Si APD detectors. A single detector is sufficient, but will only distinguish between $n = 0$ and $n > 0$ photons from the same pulse, while multiple detectors may be used in a tree to achieve partial photon-number resolution [20].[3] In addition, the contribution of such multiple pair events is significantly reduced by using a greater number of weaker pump pulses per cycle.

The storage loop as shown in figure 1 is a polarization-based system. A Pockels cell rotates the polarization of the selected photon to switch it in and out of a cavity. This storage loop only stores one polarization, the p-polarization of the PBS. The switching time is governed by the Pockels cell on-time (typically about 10 ns). The storage efficiency depends on the coatings of the relevant optical surfaces. We believe that the total loss can be reduced below 1% per pass, using carefully designed optics, such as Brewster-angle incidence for the PBS and high-quality optical coatings on the mirrors and Pockels cell. While our initial implementation will run at only 10–50 kHz, we can readily envision scaling this up above 1 MHz, e.g. using newly developed mode-locked lasers with long cavities [28].

---

[2] There are actually several possible strategies for satisfying the phase-matching, depending on the final application. For instance, one could use collinear downconversion from a type-II source [18] and separate the signal and idler photons using a PBS, or use the beacon-like output modes [19].
[3] Photon number may also be resolved with only a single detector by time-bin multiplexing [14], [21]–[24]. Also, some low-temperature detectors have demonstrated photon-number resolving capabilities [25]–[27].
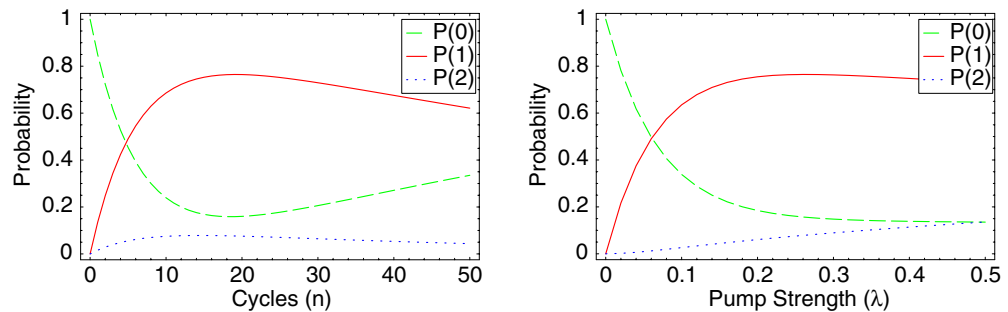
Figure 2. Efficiency of single-photon source. $P(1)$ is the probability of emitting a single photon at the output. $P(0)$ and $P(2)$ are the probabilities for failing, with 0 or $\geqslant 2$ photons (exactly two photons is by far the largest term here), respectively. These probabilities are plotted as a function of n, the number of pump pulses per attempt (left panel) and λ, the average number of emitted downconversion pairs per pulse (right panel). The baseline parameters are mean pairs per pulse $\lambda = 0.25$, number of detectors $D = 2$, storage line efficiency $\eta = 99\%$/cycle, $n = 20$ cycles and detector efficiency of $q = 70\%$. As shown, λ and n are critically important to maximize efficiency. Increasing D has only a small effect, mostly giving a small reduction in multi-photon pulses.

6. Improvements and extensions

The source described above can be used to generate a nearly deterministic source of single photons for use in quantum computing and other applications. However, there is at least one substantial improvement one can make. The detrimental effects of storage loss may be reduced by a multiple-attempts technique. In this case, we allow the storage cavity to be 'reloaded' on a later pump pulse. For instance, if we detect a single idler photon on cycle 2 of 20, there is a relatively high probability that it would be lost by the time it was to be released. However, there is also a high probability that a later cycle will also detect a single idler photon. In that case, we can discard the original signal photon and replace it with the new one. Assuming the operational parameters given in figure 2, this technique would reduce the no-photon error probability by a factor of 2. The main limitation to this technique is the ability to drive the switching Pockels cell sufficiently and quickly. However, we estimate that even allowing only two attempts can already have considerable benefit.

We can also generate signal and idler photons that are *entangled* in polarization [29, 32]. It may then be possible to couple two such single-photon sources to generate entanglement on-demand, a deterministic source of entangled pairs [30]. Finally, if the photon pairs are polarization entangled, by incorporating the methods of 'remote state preparation', described below, we could prepare the signal photon on-demand in an arbitrary quantum state.

7. Remote state preparation: theory

Remote state preparation (RSP) [31] is a quantum communication protocol that uses the correlations between two entangled systems to prepare one of them in a particular state,

conditional on the outcome of a measurement on the other. For example, if the idler photon is the trigger of our 'conditioning' source, then we can prepare the signal photon as a 'remotely prepared' qubit (RPQ) in an arbitrary quantum polarization state. We have implemented a partial scheme that remotely prepares single photons, *heralded* by the trigger photon from a two-crystal entangled source [32], with arbitrary entropy, i.e. in a controllable mixed state.

Mixed polarization states may be generated in a variety of ways [33], e.g. separating orthogonal polarizations by more than a photon's coherence length [34, 35], or tracing over one qubit of a nonmaximally entangled state [36]. Here we demonstrate a novel method of control using partial measurement [37]. Consider an initial state that is a maximally entangled: $|\phi^+\rangle \equiv (|H_t H_{rp}\rangle + |V_t V_{rp}\rangle)/\sqrt{2} \equiv (|D_t D_{rp}\rangle + |A_t A_{rp}\rangle)/\sqrt{2}$, where the subscripts label the trigger and remotely prepared photon modes. Here we have used $|H\rangle$ and $|V\rangle$ for horizontally and vertically polarized states and $|D\rangle \equiv (|H\rangle + |V\rangle)/\sqrt{2}$ and $|A\rangle \equiv (|H\rangle - |V\rangle)/\sqrt{2}$ for diagonal and antidiagonal polarizations, respectively. Measurement of the trigger photon with a diagonal (antidiagonal) polarizer (i.e. detecting the trigger photon after a polarizer) prepares the other photon in the state $|D_{rp}\rangle$ ($|A_{rp}\rangle$). If, instead, the trigger polarizer is removed, then the trigger photon is measured in a polarization-insensitive way. This is equivalent to tracing over the polarization state of the trigger photon, and remotely prepares a completely mixed state (i.e. an unpolarized photon),

$$\rho_{rp} = \langle D_t|\phi^+\rangle\langle\phi^+|D_t\rangle + \langle A_t|\phi^+\rangle\langle\phi^+|A_t\rangle$$

$$= \frac{1}{2}(|D_{rp}\rangle\langle D_{rp}| + |A_{rp}\rangle\langle A_{rp}|) = \frac{1}{2}\begin{pmatrix} 1 & 0 \\ 0 & 1 \end{pmatrix} = \rho_{mixed}. \tag{5}$$

By using a *partial* polarizer, tunable between the two proceeding cases, we can control the *strength* of the polarization measurement on the trigger and, thus, the mixedness of the other qubit. Our partial polarizer's strength is governed by the transmission of two orthogonal polarization components, T_D and T_A, normalized by $N \equiv 1/(T_D + T_A)$. Perfect transmission of one component coupled with zero transmission of the other realizes a perfect polarizer, set for the transmitted component. If $T_D = T_A$, then no polarization information is gained and the partial polarizer behaves as if no polarizer is present (although the overall amplitude may be reduced). The partial polarizer acts on the trigger, and when the trigger is used to condition the emission of the RPQ, the RPQ becomes

$$\rho_{rp}(T_D, T_A) = N(T_D\langle D_t|\phi^+\rangle\langle\phi^+|D_t\rangle + T_A\langle A_t|\phi^+\rangle\langle\phi^+|A_t\rangle)$$

$$= \frac{N}{2}(T_D|D_{rp}\rangle\langle D_{rp}| + T_A|A_{rp}\rangle\langle A_{rp}|) = \frac{1}{2}\begin{pmatrix} 1 & \alpha \\ \alpha & 1 \end{pmatrix} \equiv \rho_{rp}(\alpha), \tag{6}$$

where $\alpha = N(T_D - T_A)$. We classify the mixedness of (6) using the linear entropy $S(\rho) = 2(1 - \text{Tr}(\rho^2))$, yielding

$$S(\rho_{rp}(\alpha)) = 1 - \alpha^2. \tag{7}$$

Although near-perfect entangled states have been experimentally achieved [32], this may be difficult in some cases, especially when one is optimizing the mode collection efficiency, as in the single-photon source described above. If instead of $|\phi^+\rangle$, one starts with a non-ideal entangled
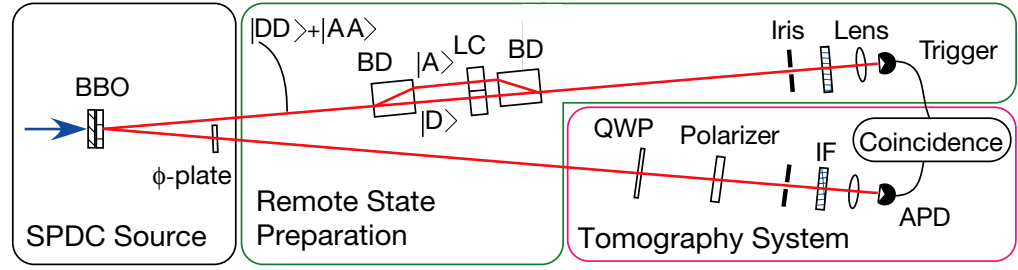
Figure 3. Experimental arrangement to remotely prepare and measure single-photon states with variable mixedness. The BBO crystals are pumped and the ϕ-plate adjusted to create an initial entangled state $(|DD\rangle + |AA\rangle)/\sqrt{2}$. The trigger photon (upper arm) enters a partial polarizer consisting of a birefringent beam displacer (BD) that separates diagonal and antidiagonal polarization components, each of which passes through a separate liquid crystal (LC), with optic axis nominally oriented vertically. The liquid crystals rotate the polarization of each path component so that the second BD variably transmits T_D and T_A (see text for details).

state of the form

$$\rho_{\phi^+}(\epsilon) = \frac{1}{2} \begin{pmatrix} 1 & 0 & 0 & 1-\epsilon \\ 0 & 0 & 0 & 0 \\ 0 & 0 & 0 & 0 \\ 1-\epsilon & 0 & 0 & 1 \end{pmatrix}, \tag{8}$$

where $|\epsilon| < 1$, then the remotely prepared state becomes

$$\rho_{rp}(\alpha, \epsilon) = \frac{1}{2} \begin{pmatrix} 1 & \alpha(1-\epsilon) \\ \alpha(1-\epsilon) & 1 \end{pmatrix}, \tag{9}$$

with linear entropy

$$S(\rho_{rp}(\alpha, \epsilon)) = 1 - \alpha^2(1-\epsilon)^2. \tag{10}$$

This model of a nonideal entangled state is useful since it is a close approximation to the entangled states that are often experimentally realized. Furthermore, we will see that $1-\epsilon$ is precisely the two-photon fringe visibility that is typically measured to check the entanglement quality.

8. Remote state preparation: experiment

We now describe an experiment utilizing the nonideal entangled state $\rho_{rp}(\alpha, \epsilon)$. The experimental apparatus consists of three steps as outlined in figure 3: creation of the initial entangled state, a partially polarizing projection of the trigger photon and a tomography of the RPQ. Frequency-degenerate 702 nm photons are generated by pumping two thin (0.6 mm thick each) BBO crystals with a cw 351 nm Ar-ion laser. Entanglement is realized by orienting the crystals such that their optic axes are in perpendicular planes so that a diagonally polarized pump creates the state

$(|HH\rangle + e^{i\phi}|VV\rangle)/\sqrt{2}$ [32]. A ϕ-plate—a half-wave plate tipped about its optic axis—is set to ensure the output state is $|\phi^+\rangle \equiv (|DD\rangle + |AA\rangle)/\sqrt{2}$. How well we are able to generate $|\phi^+\rangle$ can be represented by the two-photon fringe visibility in the diagonal–antidiagonal basis. This is measured by setting polarizers in both arms of the experiment to $\langle D|$, measuring coincidence counts, and then rotating one of the polarizers to $\langle A|$ and coincidence counting for the same amount of time. For the ideal state $|\phi^+\rangle$ there will be no $|DA\rangle$ or $|AD\rangle$ coincidences. However, if the initial state is not maximally entangled, e.g. as in $\rho_{\phi^+}(\epsilon)$, then a background of $|DA\rangle$ and $|AD\rangle$ coincidences will be detected. The level of this background can be characterized by the fringe visibility when one polarizer is kept fixed at $\langle D|$ and the second polarizer is varied. For the state $\rho_{\phi^+}(\epsilon)$, the maximum (minimum) coincidence rate will be observed when the second polarizer is along $\langle D|$ ($\langle A|$). The visibility is then given by

$$V(\rho_{\phi^+}(\epsilon)) \equiv \frac{\langle DD|\rho_{\phi^+}(\epsilon)|DD\rangle - \langle DA|\rho_{\phi^+}(\epsilon)|DA\rangle}{\langle DD|\rho_{\phi^+}(\epsilon)|DD\rangle + \langle DA|\rho_{\phi^+}(\epsilon)|DA\rangle} = 1 - \epsilon. \tag{11}$$

For the results presented below, our entangled state had $95 \pm 2\%$ visibility, i.e. $\epsilon = 5 \pm 2\%$.

In the remote state preparation stage, the trigger photon passes through a partial polarizer, an iris, and is detected by an APD. The partial polarizer is constructed using two birefringent (calcite) beam displacers (Thorlabs BD40), oriented such that, after passing through one such element, $|D\rangle$ polarized light is undeviated, whereas $|A\rangle$ polarized light is displaced by 4 mm. An identical element recombines these polarizations into the same mode (see figure 3). A multi-pixel liquid crystal (LC) is placed between the beam displacers, with a vertically oriented optic axis. The $|D\rangle$ and $|A\rangle$ beams each go through its own separately controlled LC pixel, which can rotate the polarization state according to the pixel's variable phase retardance. In the case of zero rotation, the second beam displacer transmits $|D\rangle$ polarized light undeviated as in the first case, while undoing the displacement of $|A\rangle$ polarized light so that both modes are recombined into the original spatial mode. If the LC rotates the polarized state, then only part of the beam (the original polarization component) is transmitted to the initial spatial mode; the new polarization component is directed by the second BD to a different spatial mode. At the output of the undeviated mode is an iris which screens any light that was not $|A\rangle$ ($|D\rangle$) polarized coming from the $|A\rangle$-($|D\rangle$-) polarized mode. In this way, the transmissions of the $|D\rangle$ and $|A\rangle$ polarization components may be arbitrarily adjusted. For example, suppose the LC rotated the polarization of light in the $|A\rangle$ spatial mode to $|H\rangle \equiv (|D\rangle + |A\rangle)/\sqrt{2}$; the second beam displacer will then deviate the $|A\rangle$ component so that it goes through the iris, whereas the $|D\rangle$-polarized component is transmitted undeviated and is blocked from detection by the iris. For this example, T_A=0.5. Thus, the iris selects a sub-ensemble of the trigger photons, corresponding to the transmission coefficients T_D and T_A, leaving the RPQ in the desired state.

For the rest of our discussion, the partial polarizer is treated as a black box, and is used to set the linear entropy by adjusting the relative transmissions T_D and T_A. In the ideal case, we have seen that the linear entropy is a function of the *difference* in transmission probabilities; therefore, to obtain the desired value of the RPQ's linear entropy, we fix T_D at its maximum and vary T_A:

$$T_A = T_D \frac{1 - \epsilon - \sqrt{1 - S}}{1 - \epsilon + \sqrt{1 - S}}, \tag{12}$$

where we have used the more general relation (10) to include the effects of nonmaximal initial entanglement.

The transmitted trigger photon and the remotely prepared qubit photon are each detected using photon counting avalanche photodiodes, preceded by a 1.3 mm diameter collection iris and a 2 nm FWHM interference filter (IF). Simultaneous detections within a 4.5 ns duration window are recorded as coincidences.[4] RSP requires coincidence counting because the method relies on the quantum mechanical correlations between the target photon and the prepared photon. The necessity of coincidence counting rules out any possibility of superluminal communication, as such counting cannot be done faster than the time it takes for the electronic signals from each APD to travel to the coincidence circuitry.

Since it is impossible to determine the state of an unknown quantum system with a single measurement, quantum state tomography is performed on an ensemble of identical remotely prepared qubits, using a quarter-wave plate and a rotating polarizer. The RPQ is projected into $\langle H|$, $\langle V|$, $\langle D|$ and $\langle A|$ using the polarizer; and it is projected into $\langle L|$ and $\langle R|$ (left and right circular polarizations, respectively) using the quarter-wave plate followed by the polarizer. Measuring the complete basis allows us to normalize each measurement, e.g. a normalized H measurement divides the counts from the $\langle H|$ projection by the sum of the $\langle H|$ and $\langle V|$ projection's counts.[5] In the absence of statistical fluctuations, the above normalized measurements would completely constrain the state of the system. However, fluctuations can make the state appear slightly unphysical, so a maximum likelihood technique (described in [35]) is used to find the closest physical state accounting for the data. Typically, ∼2000 counts were collected per tomography, for a total tomography counting time of 10 min. As shown in figure 4, the experimentally determined values of linear entropy agree very well with those predicted from equation (10). Error bars are generated by simulating Poisson fluctuations for the measured number of photon counts. Although the imperfect entanglement in our initial state prevented remote state preparation of a completely pure state ($S_L = 0$), we were able to realize the lowest entropy state predicted by equation (10). Here we have focused on remotely controlling the entropy of a qubit. Elsewhere, we will describe the full method to remotely prepare completely arbitrary single qubit states [38].

## 9. Arbitrary single-photon states on-demand

Combining the single-photon generation techniques with remote state preparation methods would allow the preparation of single photons in arbitrary quantum states on demand. In this case, however, the schematic shown in figure 1 must be modified. In addition to including (partial) polarization analysis in the trigger arm, the polarization state of the signal photons must be preserved by the switching elements. One possibility for a polarization-preserving switch, introduced in [12], is shown in figure 5. This particular switch still uses the photon polarization, flipping the horizontal and vertical polarizations on each cycle of the switch. In addition, to reduce the likelihood that the trigger of the remotely prepared state allows multiple photons to be stored, the output of the trigger's partial polarizer waste port would also have to be monitored. If two photons were detected anywhere in the trigger stage, switching the signal photons into the

---

[4] We estimate the probability of two photons from different pairs being detected within the same coincidence window accidentally is 5×10^{-9} per coincidence window, so the accidental rate (e.g. between photons corresponding to different pairs or detector dark counts) is negligible and has not been subtracted from the data.

[5] We normalize the measurements so that the small transmission difference between measuring with and without the quarter-wave plate is not an issue.
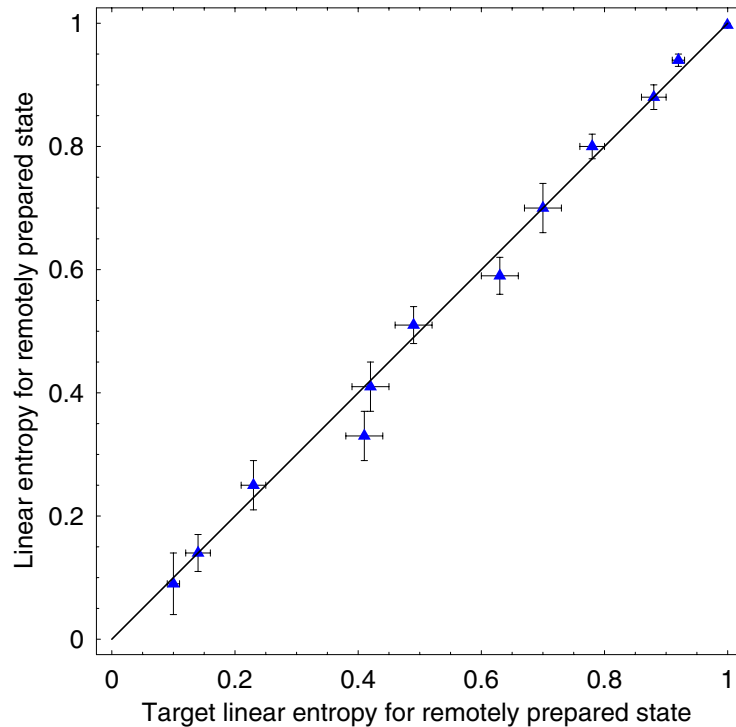
Figure 4. Linear entropy of remotely prepared states as a function of the target linear entropies. For comparison, the line $y = x$ is also shown. The target linear entropy is estimated using equation (10) by inputting the experimentally measured values for T_D, T_A, and ϵ (see text).
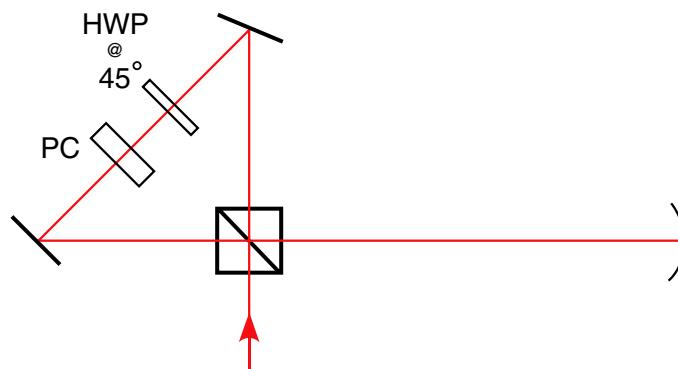
Figure 5. A polarization-preserving switch. When the Pockels cell (PC) is off, each trip through the switch rotates the horizontal polarization component to vertical and vice versa. Thus, the polarization keeps being flipped, returning to the original state after an even number of cycles. While the PC is off, any light entering will leave by the same port (either to the delay loop or back towards the downconversion crystal). Switching in and out of the storage loop is performed by applying a pulse to the PC to negate the effect of the half-wave plate, diverting the signal to the other mode.

cavity would be aborted. Note that the conditioning process reduces the probability of detecting the 'trigger' photon. However, as indicated in section 4, it should still be possible to achieve a very high probability of a single photon—now in an arbitrary (remotely prepared) state—in the output. Such a source would be a useful quantum communication resource.

Acknowledgments

References

[1] Gisin N *et al* 2002 *Rev. Mod. Phys.* **74** 145
[2] Bennett C H *et al* 1993 *Phys. Rev. Lett.* **70** 1895
[3] Nielsen M A and Chuang I L 2000 *Quantum Computation and Quantum Information* (Cambridge: Cambridge University Press)
[4] Knill E, Laflamme R and Milburn G J 2001 *Nature* **409** 46
[5] Michler P *et al* 2002 *Science* **290** 2282
      Santori C *et al* 2001 *Phys. Rev. Lett.* **86** 1502
[6] Kurtsiefer C *et al* 2000 *Phys. Rev. Lett.* **85** 290
      Brouri R *et al* 2002 *Eur. Phys. J.* D **18** 191
[7] Kuhn A, Hennrich M and Rempe G 2002 *Phys. Rev. Lett.* **89** 067901
[8] McKeever J *et al* 2004 *Science* **303** 5666
[9] Kumar P *et al* 2004 *Quantum Inform. Process.* submitted
[10] Burnham D C and Weinberg D L 1970 *Phys. Rev. Lett.* **25** 84
[11] Hong C K and Mandel L 1986 *Phys. Rev. Lett.* **56** 58
[12] Pittman T B, Jacobs B C and Franson J D 2002 *Phys. Rev.* A **66** 042303
[13] Migdall A L, Branning D and Castelletto S 2002 *Phys. Rev.* A **66** 053805
[14] Achilles D *et al* 2003 *Preprint* quant-ph/0310183
[15] Monken C H, Souto Ribeiro P H and P'adua S 1998 *Phys. Rev.* A **57** R2267
[16] Kurtsiefer C, Oberparleiter M and Weinfurter H 2001 *Phys. Rev.* A **64** 023802
[17] Bovino F A *et al* 2003 *Opt. Commun.* **227** 343
[18] Kiess T E *et al* 1993 *Phys. Rev. Lett.* **71** 3893
[19] Takeuchi S 2001 *Opt. Lett.* **26** 843
[20] Kok P and Braunstein S L 2001 *Phys. Rev.* A **63** 033812
[21] Banaszek K and Walmsley I A 2003 *Opt. Lett.* **28** 52
[22] Achilles D *et al* 2003 *Opt. Lett.* **28** 2387
[23] Fitch *et al* 2003 *Phys. Rev.* A **68** 043814
[24] Řeháĉek J *et al* 2003 *Phys. Rev.* A **67** 061801
[25] Waks E *et al* 2003 *Preprint* quant-ph/030054
[26] Kwiat P G *et al* 1994 *Appl. Opt.* **33** 1844
[27] Miller A J *et al* 2003 *Appl. Phys. Lett.* **83** 791
[28] Richardson M *Unpublished work* University Central Florida
[29] Kwiat P G *et al* 1995 *Phys. Rev. Lett.* **75** 4337
[30] Kok P, Williams C P and Dowling J P 2003 *Phys. Rev.* A **68** 022301
[31] Bennett C J *et al* 2001 *Phys. Rev. Lett.* **87** 077902
[32] Kwiat P G *et al* 1999 *Phys. Rev.* A **60** R773

Institute *of* **Physics** Φ DEUTSCHE PHYSIKALISCHE GESELLSCHAFT

[33] Kwiat P G and Englert B-G 2004 *Science and Ultimate Reality: Quantum Theory, Cosmology and Complexity* ed J D Barrow, P C W Davies and C L Harper Jr (Cambridge: Cambridge University Press) to appear
[34] Berglund A J 2000 *BA Thesis* Dartmouth College [*Preprint* quant-ph/0010001]
[35] Peters N *et al* 2003 *J. Quant. Inf. Comp.* **3** 503
[36] Ericsson M *et al* 2004 *Phys. Rev. Lett.* submitted
[37] Berry D W and Sanders B C 2003 *Phys. Rev. Lett.* **90** 057901
[38] Peters N A *et al* 2004, in preparation